1.E.3 *Nuclear Physics* A244 (1975) 1—14;

TRANSIENT FIELD MEASUREMENTS OF g-FACTORS FOR ^{28}Si AND ^{30}Si

J. L. EBERHARDT, R. E. HORSTMAN, H. A. DOUBT and G. VAN MIDDELKOOP
Fysisch Laboratorium, Rijksuniversiteit, Utrecht, The Netherlands

Received 10 March 1975

Abstract: Transient field precession measurements have been performed on the first excited $J^\pi = 2^+$ states of ^{28}Si and ^{30}Si with the IMPAC technique on recoil in magnetized iron. The results were analyzed with empirically adjusted Lindhard-Winther predictions. This yields g-factors of $g = +0.56\pm0.09$ and $g = +0.56\pm0.16$ for ^{28}Si and ^{30}Si, respectively. In the present cases the influence of static hyperfine fields is negligible due to the very short mean lives for ^{28}Si and ^{30}Si of 0.68 and 0.35 ps, respectively. The results are compared with theoretical calculations. Previous results for ^{26}Mg(2_1^+) were reanalyzed with the more recent lifetime of $\tau_m = 0.72\pm0.03$ ps. The value of the g-factor becomes $g = +0.82\pm0.16$.

E NUCLEAR REACTIONS ^{28}Si($\alpha, \alpha'\gamma$), $E = 7.50$ MeV; ^{30}Si($\alpha, \alpha'\gamma$), $E = 8.50$ MeV; measured $\alpha\gamma(\theta, B)$ in polarized Fe and Doppler-shift attenuation. ^{26}Mg($\alpha, \alpha'\gamma$); analyzed previous data. ^{26}Mg, ^{28,30}Si levels deduced g and τ_m for first 2^+ states. ^{30}Si enriched targets. IMPAC.

1. Introduction

It has been shown recently [1]) that the knowledge of electromagnetic properties of low-lying levels in doubly even $T = 1$ nuclei in the middle of the sd shell provides a sensitive test of nuclear effective interactions, since in the middle of the shell the model space gives an adequate description of the states involved.

The present paper reports the measurement of the g-factors of the first excited 2^+ states of ^{28}Si and ^{30}Si with the ion-implantation perturbed angular correlation technique [2]) (IMPAC), utilizing the transient magnetic field experienced by an ion slowing down in magnetized iron [3]). The experimental precessions were compared with the empirically adjusted Lindhard-Winther theory [3, 4]). A preliminary report has appeared in ref. [5]).

For these short-lived nuclear states the transient field precession strongly depends on the nuclear lifetime. It is thus essential to know these lifetimes accurately. An experimental comparison with recent high-precision lifetime measurements may also test the validity of the stopping power of Si in Fe used in the calculation of the transient field precession. The mean lives of ^{28}Si(2_1^+) and ^{30}Si(2_1^+) were extracted as a by-product of the present investigation from the Doppler-shift line shapes measured with a Ge(Li) detector positioned at an angle of 0° to the beam direction. The results show excellent agreement with the average values quoted in ref. [6]) and with a recent accurate measurement in this laboratory [7]).

For ^{26}Mg previous results [4]) were reanalyzed with a recent accurately measured lifetime [8]). This leads to a revision of the measured value of the g-factor of ^{26}Mg(2_1^+).

2. Experimental procedure

The 1.78 MeV level of ^{28}Si and the 2.24 MeV level of ^{30}Si were excited by inelastic scattering of α-particles obtained from the Utrecht 7 MV EN tandem accelerator. The experimental set-up, the preparation of the Fe target-backings and the data collection have been discussed in detail in an earlier publication [4]).

The coincident γ-ray yields were first measured as a function of the ^{4}He$^+$ bombarding energy in the geometry used in the g-factor measurements, i.e. γ-rays were detected with a 12.7 cm diam. by 12.7 cm long NaI(Tl) detector at 72° with respect to the beam axis in coincidence with backscattered α-particles detected between angles of 166° and 174° in an annular Si detector. For short-lived nuclear states ($\tau_m < 2$ ps) the transient field precession has a maximum value for a particular initial recoil energy [see for example fig. 10 of ref. [4])]. Since the optimum recoil energies for ^{28}Si and ^{30}Si are 1.0 MeV and 0.5 MeV, respectively, the yield measurements were limited to bombarding energies ranging a few MeV above the Coulomb

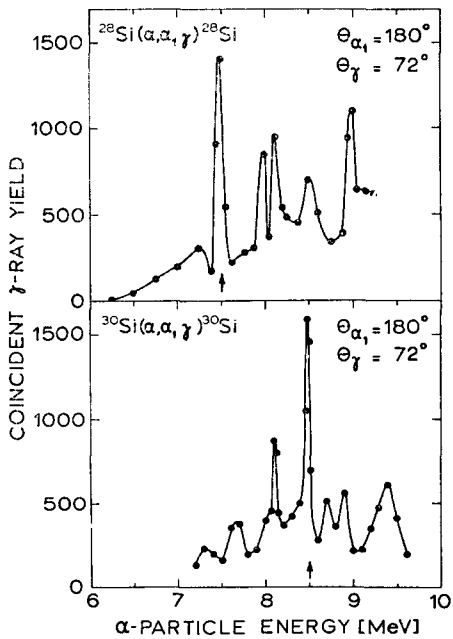

Fig. 1. Coincident γ-ray yields per 15 μC and 60 μC collected charge for ^{28}Si and ^{30}Si, respectively, as a function of α-bombarding energy. The targets consisted of 115 μg/cm^2 $^{28}SiO_2$ and 90 μg/cm^2 $^{30}SiO_2$. The lines are intended to guide the eye. The arrows indicate the energies chosen for the experiments.

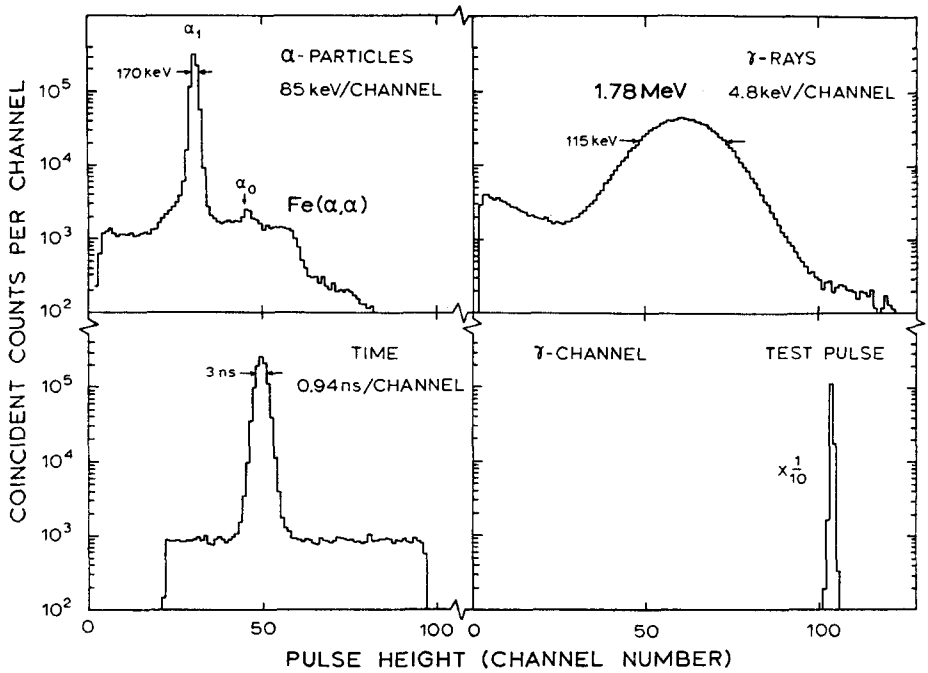

Fig. 2. Typical coincidence α-particle, γ-ray and time spectra for ^{28}Si. The γ-ray pulses were biased to reduce the counting rate in the computer with all γ-rays below 1.50 MeV rejected. In the γ-ray spectrum random coincidences have been subtracted. A coincident test pulse spectrum in the γ-channel, which checked the proper functioning of the electronics, is also shown.

barrier (7 MeV). The results are displayed in fig. 1. The energies selected for the g-factor measurements were 7.50 MeV for ^{28}Si and 8.50 MeV for ^{30}Si. This corresponds to recoil energies of 2.82 and 2.98 MeV for the two nuclei, respectively.

Targets were prepared from natural ^{28}Si and from ^{30}Si enriched † to 95.2 % by vacuum evaporation onto 10 mg/cm^2 thick pure Fe backings ††. For the ^{28}Si and ^{30}Si experiments 0.5 mm and 10 mg/cm^2 Cu backings were used, respectively. The targets of ^{28}Si on Fe and Cu had thicknesses of 170 and 290 μg/cm^2, respectively, and for the ^{30}Si targets these thicknesses were 100 and 200 μg/cm^2. The targets were positioned in an external magnetic field of 0.15 T, the direction of which was automatically reversed every 2 min. A new area of the target was exposed to the beam every 6 h to reduce possible radiation damage effects. In order to maintain good true-to-random coincidence ratios of about 40 and 10 for ^{28}Si and ^{30}Si, respectively, and to limit pulse pile-up and dead-time losses the beam current (typically 80 nA) was not allowed to exceed 100 nA.

Coincident γ-radiation was detected with four 12.7 cm diam. by 12.7 cm long NaI(Tl) detectors at angles of ±72° and ±108°. Measurements of the total precession

† Oak Ridge National Laboratory specifications.
†† Manufactured by Ventron Corp. Massachusetts, USA.

effect in Fe and of beam bending [4]) in Cu were alternated to minimize possible systematic effects. For ^{28}Si a total of 50 h was spent measuring the precession and 56 h measuring beam bending; for ^{30}Si these periods were 81 and 77 h, respectively. The total yield obtained in the photopeak for ^{28}Si was 4.5×10^5 and 5.9×10^5 counts per detector for each field direction for precession and beam bending, respectively. For ^{30}Si these numbers were both 2.5×10^5. The ^{28}Si measurement was the cleanest and fastest of the six transient field measurements carried out so far in this laboratory [refs. [4, 5, 9])]. This is illustrated by the quality of the α-particle, γ-ray and time spectra shown in fig. 2.

3. Statistical considerations and results

The mean precession angle $\Delta\theta$ can be expressed to first order by

$$\Delta\theta = \frac{1}{4}\varepsilon W(\theta) \Big/ \frac{\mathrm{d}W(\theta)}{\mathrm{d}\theta}, \tag{1}$$

where $W(\theta)$ represents the γ-ray angular correlation. The effect ε for one pair of detectors is defined as the ratio of coincident counts accumulated in the γ-ray detectors at $(\frac{1}{2}\pi \pm \theta_1)$ with the magnetic field up and down, and is given by

$$\varepsilon = \frac{N(\frac{1}{2}\pi+\theta_1)_\uparrow}{N(\frac{1}{2}\pi-\theta_1)_\uparrow} \frac{N(\frac{1}{2}\pi-\theta_1)_\downarrow}{N(\frac{1}{2}\pi+\theta_1)_\downarrow} - 1. \tag{2}$$

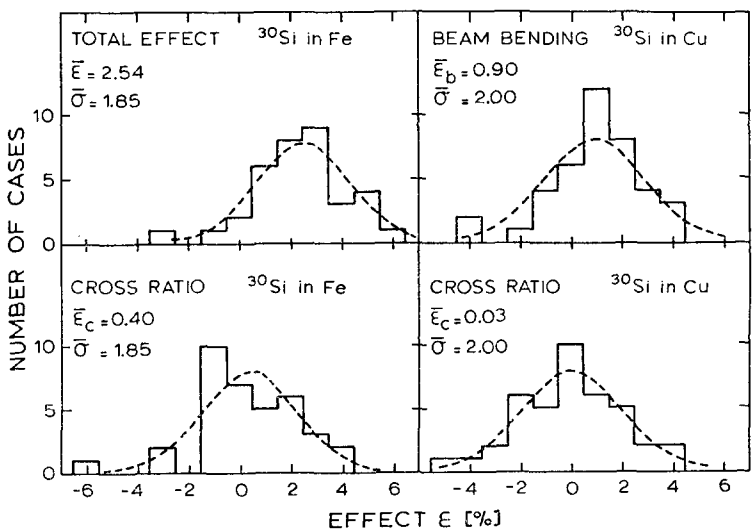

Fig. 3. Frequency distributions of the precession effects ε and cross ratios ε_c per tape for the ^{30}Si experiment. The relevant detector pairs have been summed. The expected Gaussian distributions with expectation values $\bar{\varepsilon}$ and standard deviations $\bar{\sigma}$ ($\bar{\sigma}$ is the average of the error per tape) are also shown.

TABLE 1
Summary of measured effects for ^{28}Si and ^{30}Si

Nucleus	Precession			Beam bending		
	ε [a]) (%)	ε_c [a]) (%)	$\Delta\theta_p$ (mrad)	ε [a]) (%)	ε_c [a]) (%)	$\Delta\theta_b$ (mrad)
^{28}Si	3.2±0.2	0.0±0.2	1.69±0.11	0.51±0.18	−0.02±0.18	0.27±0.09
^{30}Si	2.5±0.3	0.4±0.3	1.37±0.16	0.9 ±0.3	0.1 ±0.3	0.50±0.17

[a]) The relevant detector pairs have been summed.

The measured correlations were consistent with full alignment of the 2^+ states, i.e. only magnetic substates $m = 0$ were populated. The optimum detection angle for this correlation is $\theta_1 = 18°$ [see ref. [4])].

As a check on the data the two cross ratios ε_c, given by

$$\varepsilon_c = \frac{N(\frac{1}{2}\pi \pm \theta_1)_\uparrow}{N(-\frac{1}{2}\pi \pm \theta_1)_\uparrow} \frac{N(-\frac{1}{2}\pi \pm \theta_1)_\downarrow}{N(\frac{1}{2}\pi \pm \theta_1)_\downarrow} - 1, \tag{3}$$

were also calculated. No significant deviations from zero were observed.

Frequency distributions of the effect and cross ratios per recorded magnetic tape ($\approx$ 2 h measuring time) for both precession and beam bending measurements served as a further check on the statistics. No significant deviations from purely statistical distributions were observed. This is illustrated for ^{30}Si in fig. 3.

A summary of the measured precession and beam bending effects and of the cross ratios is given in table 1.

4. High-resolution data

4.1. CHECK ON TARGET CONDITIONS

The use of a 125 cm^3 Ge(Li) detector for the ^{28}Si experiment and a 60 cm^3 Ge(Li) detector for the ^{30}Si experiment positioned at an angle of 0° to the beam axis served three purposes:

(i) To check that the target remained in good contact with the backing throughout the measurement. Only in the case of ^{28}Si on Cu was some loss of contact detected, but since the perturbation of the angular correlation is small on recoil into vacuum at this velocity and lifetime, these data could be included in the determination of the beam bending.

(ii) To trace possible contaminant γ-rays not resolved with the NaI(Tl) detectors. In the total-coincident γ-ray spectrum of ^{30}Si a γ-ray peak at $E_\gamma = 2.31$ MeV was detected close to the peak of interest ($E_\gamma = 2.24$ MeV), see fig. 4a. This peak probably arises from the ^{14}N(α, $\alpha_1\gamma$)^{14}N reaction on a trace of N-containing glue with which the targets were fixed to the support. With proper gates on time and particle spectra

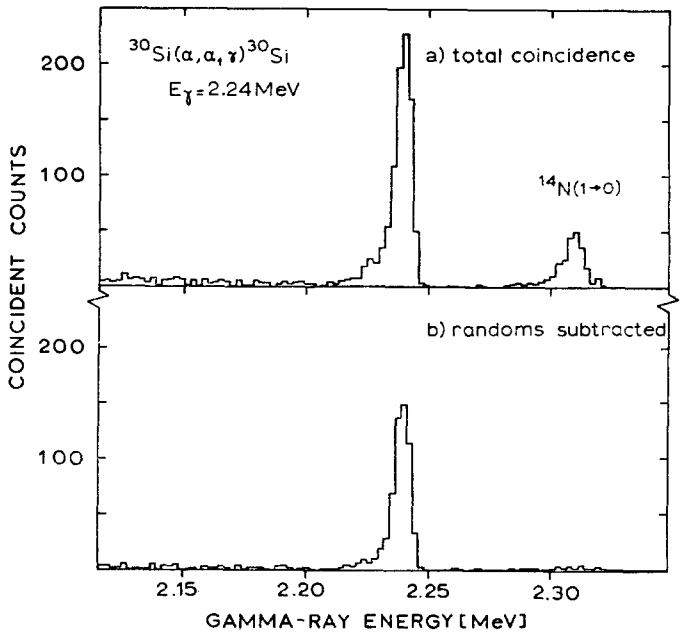

Fig. 4. Part of the Ge(Li) γ-ray spectrum for ^{30}Si with the contaminant at 2.31 MeV probably from the ^{14}N(α, $\alpha_1\gamma$)^{14}N reaction. In (a) the total coincidence spectrum is shown and in (b) the coincidence spectrum with randoms subtracted.

and after subtraction of random coincidences, however, this contaminant contributes only 4 % (see fig. 4b).

(iii) To obtain Doppler-shift line shapes for the extraction of the mean lives of the ^{28}Si and ^{30}Si first excited states.

4.2. MEAN LIFETIMES

For both ^{28}Si and ^{30}Si the theoretical Doppler-shift line shapes were fitted to the experimental data with the Utrecht linefit program LISH [ref. [7])] with the mean life τ_m of the nuclear state as a parameter. The electronic stopping powers of Si in Fe and Cu were obtained by quadratic interpolation of the stopping powers of Ti, Ni and Ge, given by the Northcliffe and Schilling tables [10]). For the stopping power of Si in Si the values for C, Al and Ti were used in the interpolation. The nuclear stopping power was approximated by $(dE/dR)_n = -K_n/(v/v_0)$ with K_n determined from Bohr's estimate [11]). For ^{28}Si the intrinsic line shape was determined with a ^{88}Y radioactive source; in the case of ^{30}Si this was estimated from the stopped fraction in the Doppler-shift line shape. Kinematic broadening and relativistic effects were included in the analysis [7]), although the influence of these effects on the mean life is negligible in the present case.

The errors in the deduced mean lives were composed of statistical errors, typically 5 %, and an independent 15 % uncertainty in the stopping power. The measured

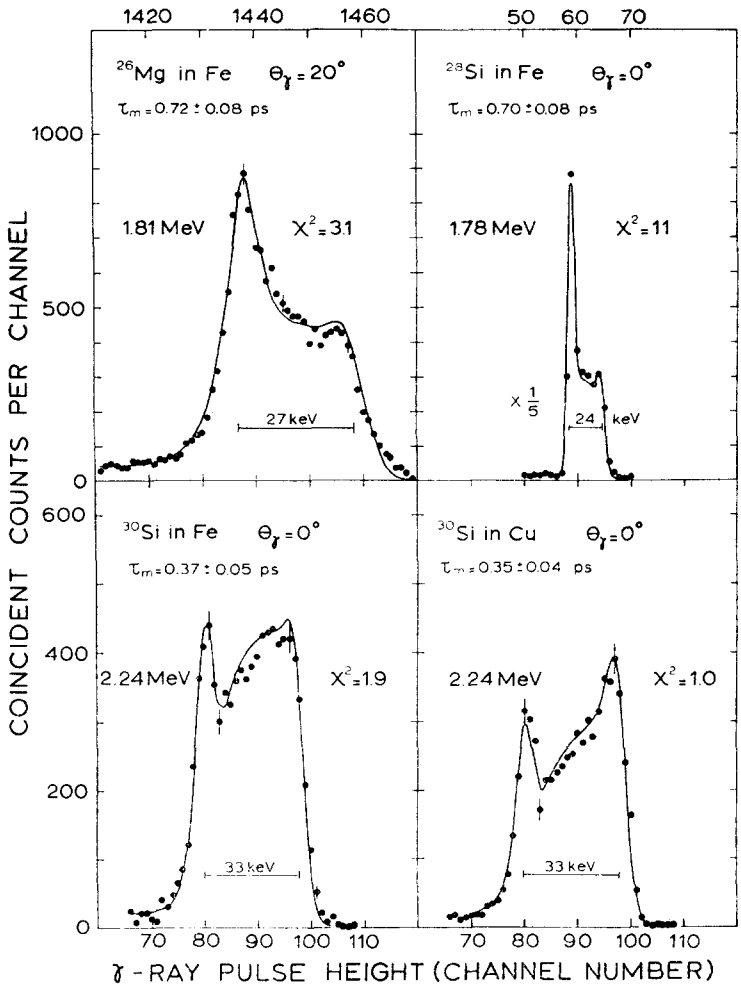

Fig. 5. Doppler-shift line shapes for the first excited states of ^{26}Mg, ^{28}Si and ^{30}Si recoiling in Fe and ^{30}Si recoiling in Cu. The curves represent least squares fits to the data.

TABLE 2

Summary of measured mean lives (in ps)

Nucleus	This work	Compilation [a]	Others
^{26}Mg(2_1^+)	0.72±0.08	0.48±0.05	0.71 ±0.08 [b] 0.72 ±0.03 [c]
^{28}Si(2_1^+)	0.70±0.08	0.68±0.03	
^{30}Si(2_1^+)	0.36±0.04	0.34±0.04	0.351±0.019 [d]

[a]) Ref. [6]). [b]) Ref. [12]). [c]) Ref. [8]). [d]) Ref. [7]).

spectra with the best fits are displayed in fig. 5, which also includes an analysis of old ^{26}Mg data [4]). In the following paragraphs the individual measurements are discussed. A summary of measured mean lives is given in table 2.

(*i*) *The ^{28}Si data.* Only the results for the Fe-backed targets were used in the analysis, because some loss of contact was observed for the Cu-backed targets (see subsect. 4.1). The poor apparent quality of the fit, $\chi^2 = 11$, is caused by non-statistical differences between the theoretical curve and the experimental points. These differences play an important role here, because for such a low dispersion the statistics per data point are extremely good. A small inadequacy in the stopping power or a small differential non-linearity of the analog-to-digital converter for example, could account for the discrepancy. The result, $\tau_m = 0.70 \pm 0.08$ ps is in excellent agreement with the average value of 0.68 ± 0.03 ps compiled by Endt and Van der Leun [6]) and this latter value was therefore used in the g-factor analysis.

(*ii*) *The ^{30}Si data.* The difference in line shape between the Fe- and Cu-backed targets (see fig. 5) mainly arises from the difference in target thickness (see sect. 2). The results of both measurements, 0.37 ± 0.05 and 0.35 ± 0.04 ps, respectively, show excellent agreement with the compiled [6]) value of 0.34 ± 0.04 ps.

Recently the mean life of the first excited state of ^{30}Si has been measured in this laboratory [7]) with the ^{3}H(^{28}Si, p)^{30}Si reaction at $E(^{28}\text{Si}) = 33$ MeV leading to recoil into Cu at $v/c = 4.79\,\%$. The result $\tau_m = 0.351 \pm 0.019$ ps is the most accurate value to date and is consistent with the present results. This value was used in the g-factor analysis.

(*iii*) *The ^{26}Mg data.* In a previous measurement [4]) of the g-factor of the first excited state of ^{26}Mg a mean life of 0.48 ± 0.05 ps for the state was taken from the compilation [6]). A recent value of 0.71 ± 0.08 ps [ref. [12])], however, led to a later, careful off-line analysis of the Ge(Li) data. The result is shown in fig. 5. The tail between the stopped peak and the flight fraction and the tail on the right hand side of the flight fraction were not completely reproduced by the linefit program such that a rather poor χ^2 value of 3.1 was obtained. This is due to the difficulty of taking geometrical smearing into account for a detector at $\theta_\gamma = 20°$.

It was not found possible to fit the data for the Cu-backed targets reliably with the known (400 μg/cm^2) thickness of the targets. The fact that the best fit was found for a thickness of 200 μg/cm^2 indicates that this difficulty probably arises from the resonant character of the yield curve. For the 200 μg/cm^2 Fe-backed targets this difficulty did not appear. The value of 0.72 ± 0.08 ps is supported by a recent value of 0.72 ± 0.03 ps found at Brookhaven [8]) by using heavy-ion Coulomb excitation.

5. Analysis and results

5.1. THE TRANSIENT FIELD

In the analysis of the precession data, the knowledge of the transient field is essential. In ref. [4]) it was shown that the experimental transient field precessions in the

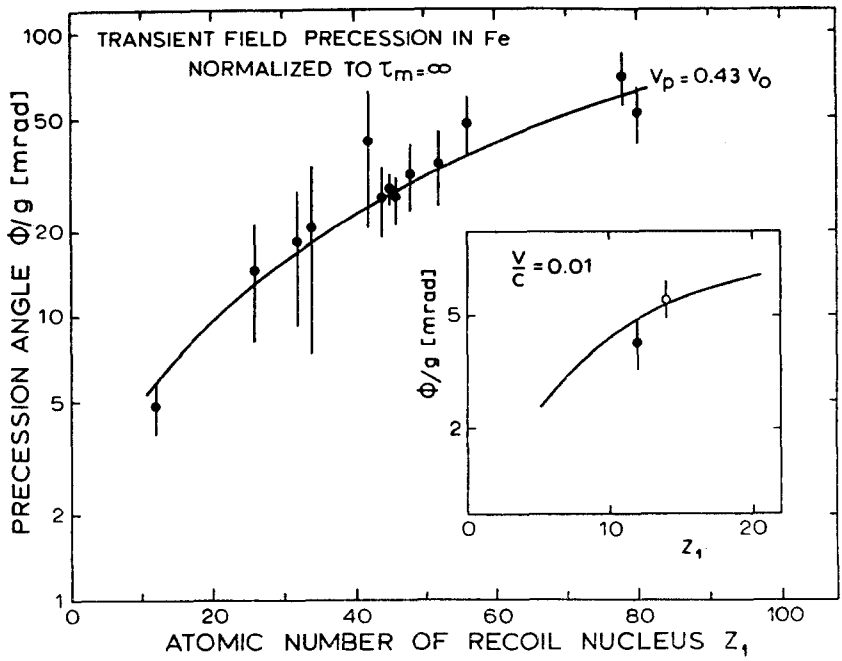

Fig. 6. The precession angle divided by the nuclear g-factor for implantation in iron, as a function of atomic number of the recoiling nucleus, normalized to recoil velocities from inelastically backscattered 33 MeV ^{16}O and infinite lifetime. The curve fitted to the experimental data ($v_p/v_0 = 0.43$) is also shown. For the experimental points with $Z_1 \geqq 26$ see ref. [4]); for the ^{24}Mg point see subsect. 5.1. The insert shows the ^{24}Mg point and the fitted curve for $Z \leqq 20$ normalized to a recoil velocity of $v/c = 0.01$. The open circle represents the measured precession for ^{28}Si divided by the average of the theoretically calculated g-factors. This point has *not* been used in the fit.

mass region $A \geqq 54$ are about a factor of two larger than those theoretically predicted [ref. [3])]. To overcome this difficulty the polarized electron velocity v_p was treated as an effective parameter and fitted to all known transient field data. This yielded $v_p/v_0 = 0.40 \pm 0.08$ [ref. [4])]. Recently the g-factor of ^{24}Mg has been measured with the time-differential deorientation technique [13]). The result $|g| = 0.51 \pm 0.02$ compared with the value of ref. [4]), $g = +0.42 \pm 0.09$, can be used to calibrate the transient field for Mg recoiling into Fe. On inclusion of ^{24}Mg in the fit one obtains $v_p/v_0 = 0.43 \pm 0.07$. Fig. 6 shows the transient field data, normalized to recoil velocities from inelastic scattering of 33 MeV ^{16}O, together with the fitted curve. For light nuclei such a normalization would lead to very high recoil velocities, where the electronic stopping power no longer follows the $\sqrt{E}$ law. The insert in fig. 6 shows the transient field precession normalized to a velocity of $v/c = 0.01$ for $A < 40$. In the fit of v_p to the data, however, the experimental precessions were compared with the theoretical values, calculated for the actual recoil velocities used in the experiments. This is important because the dependence of the precession on v_p is velocity dependent.

5.2. THE ^{28}Si AND ^{30}Si g-FACTORS

The g-factors were deduced from the experimental data with the use of the Utrecht program GFAC, which is based on eq. (11) of ref. [4]) and which takes into account the finite target thickness. The error propagation was also calculated with the program. The resulting relative errors in the g-factors produced by the statistical uncertainty

TABLE 3

Sources of errors and their contributions to the error in the g-factors

Quantity [a])	^{28}Si		^{30}Si	
	relative error (%)	contribution to g (%)	relative error (%)	contribution to g (%)
$\Delta\theta$	11	11	28	28
τ_m	4.4	3.3	5.4	6.5
v_p	16	6.1	16	4.3
$d\varepsilon/d\rho$	15	6.1	15	1.2
d	30	6.1	30	6.1
ζ	5	5	5	5
B_s		3.8		1.1
		total error 17 %		total error 30 %

[a]) The symbols are explained in subsect. 5.2.

TABLE 4

Summary of measured g-factors

Nucleus	Net precession angle (mrad)	g-factor
^{28}Si	1.42±0.15	+0.56±0.09
^{30}Si	0.9 ±0.2	+0.56±0.16
^{26}Mg	1.7 ±0.3 [a])	+0.82±0.16 [b])

[a]) From ref. [4]).
[b]) Revised value, see subsect. 5.3.

in the measured precession angle $\Delta\theta$ and by uncertainties in the nuclear lifetime τ_m, the polarized electron velocity v_p, the stopping power $d\varepsilon/d\rho$, the target thickness d, the number of polarized electrons per Fe atom ζ and the static magnetic hyperfine field B_s are given in table 3. The static magnetic hyperfine field for Si implanted in magnetized Fe is not known, but is believed from systematics [14]) to be smaller in magnitude than 10 T. This yields uncertainties of 3.8 % and 1.1 % for ^{28}Si and ^{30}Si, respectively. The total errors in the g-factors of ^{28}Si and ^{30}Si are thus 17 and 30 %, respectively. The values of the g-factors for ^{28}Si(2_1^+) and ^{30}Si(2_1^+) are $g = +0.56\pm 0.09$ and $g = +0.56\pm0.16$, respectively (see table 4).

5.3. THE ^{26}Mg g-FACTOR

The previous ^{26}Mg data [4]) were reanalyzed with the best value known for the mean life of the first excited state, ($\tau_m = 0.72 \pm 0.03$ ps, see subsect. 4.2) together with the better v_p value of $v_p/v_0 = 0.43 \pm 0.07$ (see subsect. 5.1). In the error of the g-factor the contributions from uncertainties in v_p and the stopping power are more important now then previously, as a consequence of the longer lifetime, whereas the uncertainties in target thickness and mean life are less important.

The new value derived for the g-factor is $g = 0.82 \pm 0.16$.

6. Theoretical discussion and conclusions

6.1. THEORETICAL DISCUSSION

The experimental values of the g-factors of the first excited states of ^{26}Mg, ^{28}Si and ^{30}Si are compared with some theoretical calculations in table 5. As pointed out in ref. [1]) the g-factors of the first excited states of doubly even $T = 0$ nuclei are not very sensitive to the interaction used nor to the size of the configuration space. This is demonstrated by ^{20}Ne [ref. [15])], ^{24}Mg [ref. [1])] and ^{28}Si [ref. [15])], for which excellent agreement with experimental values [refs. [4, 13]) and present work] is obtained by a Hartree-Fock calculation [16]), by free-parameter fits of the two-body matrix elements

TABLE 5

Comparison of theoretical g-factors with experiment [a])

	g-factor			
	^{26}Mg [b])		^{28}Si	^{30}Si
Experiment	$+0.82 \pm 0.16$		$+0.56 \pm 0.09$	$+0.56 \pm 0.16$
$1d_{\frac{5}{2}}2s_{\frac{1}{2}}$ configurations [c]) (full space)				
MSDI	+0.91	(0.20)	+0.54	
FPSDI	+0.89	(0.18)	+0.54	
$1d_{\frac{5}{2}}2s_{\frac{1}{2}}1d_{\frac{3}{2}}$ configurations [d])				
MSDI truncated	+0.55	(0.05)	+0.53 [e])	+0.81 [e])
ASDI truncated [f])	+0.97	(0.22)		
MSDI full space	+0.49			
Kuo truncated	+0.56	(0.01)		
Kuo full space	+0.47			
PW truncated	+1.3	(0.54)		+0.03 [e])
PW full space	+0.85			
Projected Hartree-Fock [g])	+0.53		+0.55	

[a]) The abbreviations of the interactions are explained in subsect. 6.1.
[b]) The quantity in brackets is α^2, which represents the population probability of the $\pi^{-2}(d_{\frac{5}{2}})$ state.
[c]) Ref. [17]).
[d]) Ref. [1]), unless indicated otherwise.
[e]) Ref. [15]).
[f]) Ref. [21]).
[g]) Ref. [16]).

(FPSDI) in a $1d_{\frac{5}{2}}\,2s_{\frac{1}{2}}$ configuration [17]), and by shell-model calculations with an effective two-body interaction (MSDI) in a configuration space limited to $1d_{\frac{5}{2}}\,2s_{\frac{1}{2}}$ [ref. [17])] and $1d_{\frac{5}{2}}\,2s_{\frac{1}{2}}\,1d_{\frac{3}{2}}$ [ref. [15])] shells (see table 5 for the ^{28}Si calculations). This impressive agreement provides some confidence that the theoretical values are correct and may also serve as a check on new experimental techniques, enabling, for example, a test of the transient field systematics.

Doubly even $T = 1$ nuclei such as ^{26}Mg, ^{30}Si and ^{34}S in the middle of the sd shell, on the other hand, do provide a sensitive test of nuclear interactions [1]). Various theoretical calculations for ^{26}Mg and ^{30}Si are presented in table 5.

(*i*) *The ^{26}Mg calculations.* Calculations in a full sd space [1]) and in a configuration space truncated with the "diagonal energy truncation" (DET) method [15, 18]) with both the MSDI [19]) and the Kuo [19]) interactions yield values for the g-factor, which are lower than experiment by about two standard deviations. The same discrepancy occurs for a Hartree-Fock calculation [16]). A calculation in the full sd configuration space with the Preedom and Wildenthal interaction (PW) [20]) gives excellent agreement. The above comparison suggests that the PW matrix elements, which have been derived by empirically modifying Kuo matrix elements in the full sd space to obtain improved excitation energies in the $A = 18$–22 mass region, are well able to describe heavier nuclei. The same matrix elements used in a calculation in a DET truncated space [15]), however, yield a g-factor which is three standard deviations too high.

In a recent calculation [21]) of the g-factor of ^{26}Mg(2_1^+) the empirical interaction MSDI was used, modified by a fit to excitation energies in the mass region $A = 24$–28 with a procedure similar to that of Preedom and Wildenthal. The result of "adjusted surface delta interaction" (ASDI) calculations, which also reproduce much better than MSDI the experimental excitation energies, spectroscopic factors and transition rates, agrees well with experiment.

For MSDI and FPSDI calculations limited to the $1d_{\frac{5}{2}}\,2s_{\frac{1}{2}}$ shells good agreement is also obtained.

The measure of agreement is strongly correlated with the population of the configuration with two proton holes in the $d_{\frac{5}{2}}$ shell $[\pi^{-2}(d_{\frac{5}{2}})]$. This configuration gives a major contribution to the g-factor; a pure $\pi^{-2}(d_{\frac{5}{2}})$ configuration would result in $g = +1.9$. In table 5 the α^2 values are shown for ^{26}Mg. The calculations in the full sd configuration space are performed in the m-coupling scheme [23]) and α^2 is not given. Table 5 shows that the measured value of the g-factor is reproduced by $\alpha^2 \approx 0.2$. For lower (higher) α^2 values the calculated g-factor is too low (too high).

(*ii*) *The ^{30}Si calculations.* Only two calculations have at present been carried out. An MSDI calculation in a truncated $1d_{\frac{5}{2}}\,2s_{\frac{1}{2}}\,1d_{\frac{3}{2}}$ space [15]) yields a value for the g-factor, which is somewhat too large, whereas a calculation in the same configuration space, but with the Preedom and Wildenthal (PW) interaction, gives a value for the g-factor that is lower than experiment by more than three standard deviations. This might arise from the fact that the PW matrix elements have been derived in the $A = 18$–22 mass region, where matrix elements with $d_{\frac{5}{2}}$ and $s_{\frac{1}{2}}$ configurations domi-

nate. It is not surprising that in the upper part of the sd shell, where $d_{\frac{1}{2}}$ contributions become important, poor agreement is obtained [22]). Part of the discrepancy, however, could also be caused by the truncation procedure. Table 5 shows that for ^{26}Mg the g-factor is sensitive to truncation when the PW interaction is used. Hence in the case of ^{30}Si there is a need for calculations in the full sd configuration space employing different interactions.

6.2. CONCLUSIONS

Since the publication of the initial paper [4]) demonstrating the feasibility of transient field precession measurements of nuclear g-factors in the low mass region ($A < 54$), seven new measurements have been performed, both in this laboratory [refs. [5, 9]) and present work] and elsewhere [24, 25]). This establishes the usefulness of the method for short-lived states in light nuclei.

It has been recently suggested [24, 25]) that the transient field for some low-A ions (N and O) could be more than twice as large as the empirically adjusted Lindhard-Winther calculation. For the long-lived states involved ($\tau_m > 2.6$ ps), however, one does not necessarily have to conclude a discrepancy in the transient field if static fields of the order of 10 T are present. In the present measurement the lifetime of the first excited state of ^{28}Si is short enough for the static field to be negligible and the agreement with the doubly even ($T = 0$) predictions shows no sign of a discrepancy greater that 20 % in the transient field. Further, for ^{24}Mg for which, although the lifetime of the state is longer (1.8 ps), the static field of $|B| \leqq 6$ T [from systematics [4])] results only in a 5 % correction, the empirically adjusted transient field leads to excellent agreement with another g-factor measurement [13]). Thus there seems to be good evidence that the transient field systematics are correct, at least for ions down to $Z = 12$.

Note added in proof: A very recent investigation [26]) of the transient field of ^{28}Si in Fe shows an anomalous increase in the measured precession with initial recoil velocity. This is probably caused by capture of polarized Fe electrons into 2s vacancies in the moving ion. The excellence of the ^{28}Si and ^{24}Mg results discussed above, however, gives confidence that at this low velocity the ^{30}Si and ^{26}Mg results obtained with the empirically adjusted Lindhard-Winther normalization are correct.

The authors wish to express their gratitude to J. A. Reinders (Natuurkundig Laboratorium, Universiteit van Groningen) for preparing the ^{30}Si targets. They also thank J. E. Koops and J. F. A. van Hienen for many fruitful discussions. One of us (H.A.D.) is grateful to the "Stichting voor Fundamenteel Onderzoek der Materie" (F.O.M.) for a honorarium. This work was performed as a part of the research program of F.O.M. with financial support from the "Nederlandse Organisatie voor Zuiver Wetenschappelijk Onderzoek" (Z.W.O.).

References

1) P. W. M. Glaudemans, J. E. Koops, F. Meurders and B. J. Cole, Proc. Int. Conf. on nuclear structure and spectroscopy, Amsterdam, 1974, vol. 2, p. 107
2) L. Grodzins, Hyperfine structure and nuclear radiations, ed. E. Matthias and D. A. Shirley (North-Holland, Amsterdam, 1968) p. 607
3) J. Lindhard and A. Winther, Nucl. Phys. **A166** (1971) 413
4) J. L. Eberhardt, R. E. Horstman, H. W. Heeman and G. van Middelkoop, Nucl. Phys. **A229** (1974) 162
5) R. E. Horstman, J. L. Eberhardt, H. A. Doubt and G. van Middelkoop, Proc. Int. Conf. on nuclear structure and spectroscopy, Amsterdam, 1974, vol. 1, p. 136
6) P. M. Endt and C. van der Leun, Nucl. Phys. **A214** (1973) 1
7) J. A. J. Hermans *et al.* (Utrecht), to be published
8) D. Schwalm *et al.*, as quoted by E. K. Warburton, Proc. Int. Conf. on nuclear structure and spectroscopy, Amsterdam, 1974, vol. 2, p. 506
9) J. F. A. van Hienen, thesis, Utrecht, 1975
10) L. C. Northcliffe and R. F. Schilling, Nucl. Data Tables **7** (1970) 233
11) E. K. Warburton, J. W. Olness and A. R. Poletti, Phys. Rev. **160** (1967) 938
12) M. A. Ali, J. R. Coffin, P. Wagner and G. Gallman, Proc. Int. Conf. on nuclear structure and spectroscopy, Amsterdam, 1974, vol. 1, p. 124
13) R. E. Horstman, H. A. Doubt, J. L. Eberhardt and G. van Middelkoop, Nucl. Phys., to be published
14) H. de Waard, see F. van der Woude and G. A. Sawatzky, Phys. Rep. **12C** (1974) 336
15) J. E. Koops (Utrecht), private communication
16) M. R. Gunye, Phys. Lett. **37B** (1971) 125
17) J. F. A. van Hienen, P. W. M. Glaudemans and J. van Lidth de Jeude, Nucl. Phys. **A225** (1974) 119
18) J. E. Koops, J. P. L. Reinecke and P. W. M. Glaudemans, Proc. Int. Conf. on nuclear structure and spectroscopy, Amsterdam, 1974, vol. 1, p. 23
19) E. C. Halbert, J. B. McGrory, B. H. Wildenthal and S. P. Pandya, Adv. in Nucl. Phys. **4** (1971) 316
20) B. M. Preedom and B. H. Wildenthal, Phys. Rev. **C6** (1972) 1633
21) F. Meurders, P. W. M. Glaudemans, J. F. A. van Hienen and G. A. Timmer, to be published; G. A. Timmer *et al.* (Utrecht), in preparation
22) B. J. Cole, A. Watt and R. R. Whitehead, J. of Phys. **A7** (1974) 1374
23) R. R. Whitehead, Nucl. Phys. **A182** (1972) 290
24) M. Forterre, J. Gerber, J. P. Vivien, M. B. Goldberg, K.-H. Speidel and P. N. Tandon, Phys. Rev. C, submitted
25) M. Forterre, J. Gerber, J. P. Vivien, M. B. Goldberg and K.-H. Speidel, Phys. Lett. **55B** (1975) 59
26) J. L. Eberhardt, G. van Middelkoop, R. E. Horstman and H. A. Doubt, Phys. Lett. **B**, to be published